CHEMISTRY OF MATERIALS

Article

pubs.acs.org/cm

How Dopants Can Enhance Charge Transport in Li_2O_2

Maxwell D. Radin,[†] Charles W. Monroe,[‡] and Donald J. Siegel*[,§]

[†]Department of Physics, [‡]Department of Chemical Engineering, and [§]Department of Mechanical Engineering, University of Michigan, Ann Arbor, Michigan 48109, United States

Supporting Information

ABSTRACT: The performance of high-capacity Li/O_2 batteries is limited by the high overpotential associated with the oxygen evolution reaction (OER) during charging. These losses have been attributed to sluggish charge transport within the solid lithium peroxide (Li_2O_2) discharge phase. Recent experiments have shown that use of Co_3O_4-containing Li/O_2 electrodes enhances rechargeability, but the mechanism responsible for this effect is unclear, as are the general prospects for the promotion of the Li/O_2 OER. Here first-principles calculations are combined with continuum-scale transport theory to build a multiscale model which demonstrates that the incorporation of trace Co into Li_2O_2 is a plausible mechanism for OER promotion. These calculations suggest that doping at equilibrium levels (tens of ppm) can enhance charge transport by shifting the balance of Li-ion vacancies and hole polarons. This mechanism could rationalize the improved rechargeability observed in Li/O_2 electrodes containing Co. On the basis of a computational assessment of 22 additional dopants, we speculate that Ni may also be an effective OER promoter.

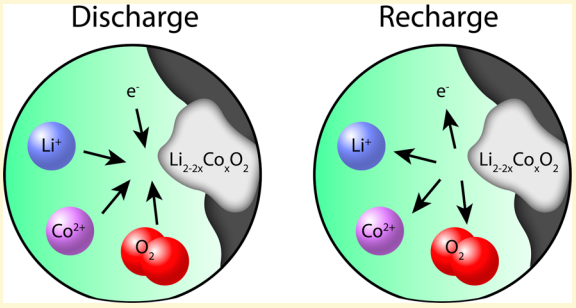

1. INTRODUCTION

Li/O_2 batteries are attracting attention as a high-capacity, and potentially low-cost, energy-storage technology.[1−4] Several important performance gaps must be resolved before these systems become commercially viable, however. Perhaps the most significant of these challenges is the high overpotential required to drive the recharging process, which is an oxygen evolution reaction (OER) associated with the decomposition of the solid lithium peroxide (Li_2O_2) discharge product. Many studies have employed additives intended to reduce OER overpotentials, but the specific role these materials play is unclear.[1,4−10] Although additives are often referred to as "catalysts", it appears unlikely that they function as true electrocatalysts for the OER, given that (i) conventional catalysts would presumably become buried by Li_2O_2 during discharge and rendered inactive,[5] and (ii) prior studies have found kinetics of the OER to be facile on typical substrates without additives present.[11]

A recent study by Black et al. demonstrated the ability of Co_3O_4-containing electrodes to promote the oxidation of thick Li_2O_2 deposits in a Li/O_2 cell.[9] The charge plateau for these electrodes was approximately 400 mV lower than in carbon electrodes, despite the fact that the presence of Co_3O_4 did not appear to influence the Li_2O_2 morphology (which is known to affect charging potentials[12−17]) or contribute significantly to electrolyte oxidation. Since the effect could not be attributed to catalysis, the term "promoter" was suggested.[9] (Henceforth we adopt the same nomenclature to refer to a compound that reduces the overpotentials of a Li/O_2 cell by a mechanism besides catalysis.) It was speculated that the promotion of the OER arose from an enhancement in surface transport of Li_xO_2 species, or possibly the scavenging of nascent oxygen. Additional studies have found Li/O_2 electrodes containing Co_3O_4[18−22] and Co-containing compounds[23,24] to exhibit improved performance.

Several mechanisms have been hypothesized to justify observations that Li/O_2 electrode additives reduce cell potentials during charging.[1,5,9,10,12−17,25−27] Despite the abundance of proposed explanations, the mechanism by which a given promoter functions remains an open question. Motivated by the experiments of Black et al.,[9] this paper explores the possibility and consequences of Co incorporation as a substitutional dopant within the Li_2O_2 discharge product. More specifically, a multiscale model is developed to evaluate the effects of Co doping on the transport properties of Li_2O_2, by combining first-principles calculations with a continuum transport model.

Charge-transport limitations through Li_2O_2 are thought to contribute significantly to charging overpotentials.[3,10,28−30] Consequently, it is hypothesized here that the incorporation of impurities may enhance Li_2O_2 oxidation by improving the conductivity associated with hole polarons and/or Li-ion vacancies. Although we are not aware of experimental efforts to quantify the incorporation of metal dopants within the discharge product, we speculate that this "in situ doping" could occur via diffusion of Co ions into the discharge product during its growth, or through the incorporation of trace Co ions that are dissolved in the electrolyte. The latter possibility is

Received: October 20, 2014
Revised: December 30, 2014
Published: December 31, 2014

DOI: 10.1021/cm503874c
Chem. Mater. 2015, 27, 839−847

supported by the observed dissolution of Co into the electrolyte in Li-ion batteries using Co-based electrodes.[31] The electrochemical incorporation of additives has been exploited in other contexts, such as the electrodeposition of metals[32] and the formation of tailored solid−electrolyte interphases in Li-ion batteries,[33] motivating the concept of doping Li_2O_2 in situ. Indeed, experiments on Li/O_2 cells have shown that halide species from the electrolyte are incorporated into the discharge product.[34]

To investigate the feasibility and consequences of in situ doping of Li/O_2-battery discharge products, the thermodynamics of Co substitutions in Li_2O_2 is analyzed computationally; this data is subsequently used to parametrize a continuum model that demonstrates the impact of doping on transport within a Li_2O_2 film.

Our model reveals that Co substitutions can significantly enhance charge transport in Li_2O_2. For example, if Co is incorporated at equilibrium levels (13 ppm), the transport model predicts that only ∼10 mV of potential is needed to drive a 1 $\mu A/cm^2$ current density through a 100 nm film. This contrasts strongly with undoped Li_2O_2, which we previously predicted to be highly resistive, requiring overpotentials of ∼1 V to drive appreciable currents.[28] Such an enhancement of transport properties by doping is consistent with the well-known impact of point defects on solid-state charge and mass transport processes.[35,36] Although the present multiscale model focuses on rationalizing recent experiments involving Co-containing Li/O_2 electrodes,[9] it is reasonable to hypothesize that the mechanism proposed here could also explain the impact of other promoters on the OER from Li_2O_2.[7,8,20,37] To explore this possibility, 22 additional dopants were computationally screened. The low formation energy calculated for Ni substitutions suggests that Ni-containing compounds could also be effective promoters.

2. DEFECT CHEMISTRY

It is first necessary to determine the expected equilibrium concentration of Co dopants within the Li_2O_2 discharge phase. Although the defect chemistry of oxides has been extensively studied, peroxides have received much less scrutiny;[27−29,38−42] the limited availability of experimental data for these compounds motivates our use of first-principles methods for calculating these properties. In a previous investigation of the intrinsic defect chemistry and conductivity of Li_2O_2,[28] it was determined that the dominant intrinsic charge carriers are hole polarons and negative lithium vacancies; a recent experimental study also independently arrived at the same conclusion.[29]

The introduction of Co dopants within the Li_2O_2 discharge phase can shift the equilibrium concentrations of intrinsic defects as follows. For a defect of type k, the equilibrium concentration c_k^0 depends upon the formation energy E_k^0 and the number density of defect sites M_k:[43]

$$c_k^0 = M_k e^{-E_k^0/k_B T} \quad (1)$$

The formation energies for Co substitutions in Li_2O_2 were calculated using the Heyd−Scuseria−Ernzerhof (HSE) functional[44,45] as implemented in the Vienna ab initio simulation package (VASP)[46−49] with 144-atom supercells and Γ-point-only k-space integration. An HSE mixing parameter of $\alpha = 0.48$ was used, since this was previously found to reproduce the GW band gap of Li_2O_2.[28] Details of the computational method (including finite-size[50] and oxygen-overbinding corrections,[51−53] and results obtained with a smaller mixing parameter of $\alpha = 0.25$) can be found in the Supporting Information and in our prior report.[28]

The formation energies and equilibrium concentrations of defects depend on the chemical potentials of Li, O, and Co. These chemical potentials are taken to be fixed by the three-phase equilibrium between Li_2O_2, O_2, and $LiCoO_2$. As discussed in the Supporting Information, this represents equilibrium in a Li/O_2 electrode that contains enough Co to saturate the Li_2O_2, i.e., to reach the solubility limit within the peroxide phase. (As shown below, the Co doping levels needed to reach saturation are quite low.) Using Co_3O_4 instead of $LiCoO_2$ as the Co reservoir would result in an even larger equilibrium concentration of Co dopants in Li_2O_2. This would represent a metastable state, however, as the Li−Co−O phase diagram shows that the reaction of Co_3O_4 and Li_2O_2 to form $LiCoO_2$ and O_2 is spontaneous. To avoid complications associated with the energies of oxides yielded by density functional theory (DFT) calculations,[54] the chemical potential for Co was determined by combining a first-principles calculation on ferromagnetic hcp Co metal with the experimental formation free energy of $LiCoO_2$;[55] see the Supporting Information for details.

Substitution of Co on Li sites was considered for the two common charge states of Co:[56] Co^{2+} and Co^{3+}. These substitutions are notated here as Co_{Li}^{+} and Co_{Li}^{2+}, respectively, where the superscript refers to the net charge of the defect, not the charge state of the Co ion. Substitution-vacancy complexes $Co_{Li}^{2+}-V_{Li}^{-}$ and $Co_{Li}^{+}-V_{Li}^{-}$ were also considered. Since there are two symmetry-inequivalent Li sites [trigonal prismatic (TP) and octahedral (Oct)], the total number of extrinsic defects considered is 12: two Co_{Li}^{+}, two Co_{Li}^{2+}, four $Co_{Li}^{+}-V_{Li}^{-}$, and four $Co_{Li}^{2+}-V_{Li}^{-}$ sites.

Figure 1 shows the calculated formation energies of the most stable of these 12 substitutional defects, as well as the formation energies of the dominant charged intrinsic defects:[28] Li-ion vacancies (V_{Li}^{-}) and hole polarons (p^+). Equilibrium formation energies and concentrations (with the Fermi level set by electroneutrality in the presence of Co) are listed in Table 1. The computations indicate that Co ions in Li_2O_2 favor the +2 charge state over the +3 charge state and prefer the Oct Li site

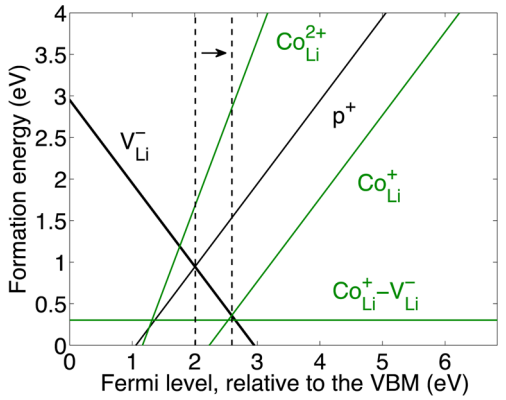

Figure 1. Calculated formation energies of Co impurities, negative Li vacancies, and hole polarons in Li_2O_2. The horizontal axis shows the Fermi level relative to the valence band maximum (VBM); vertical dotted lines show the shift in equilibrium Fermi level induced by incorporating Co impurities. Only the lowest-energy extrinsic defect for each charge state is shown.

DOI: 10.1021/cm503874c
Chem. Mater. 2015, 27, 839−847

Table 1. Equilibrium Formation Energies and Concentrations of Co Substitutions and Intrinsic Defects in Li_2O_2

defect	E_k^0 (eV)	c_k^0 (cm^{-3})
p^+	1.54	1×10^{-3}
V_{Li}^-(Oct)	0.36	2×10^{16}
V_{Li}^- (TP)	0.34	5×10^{16}
Co_{Li}^+(Oct)	0.36	7×10^{16}
Co_{Li}^+ (TP)	1.38	7×10^{-1}
Co_{Li}^{2+} (Oct)	2.86	3×10^{-26}
Co_{Li}^{2+} (TP)	3.16	3×10^{-31}
Co_{Li}^+(Oct)−V_{Li}^- (Oct)	0.42	1×10^{16}
Co_{Li}^+(Oct)−V_{Li}^- (TP)	0.30	2×10^{18}
Co_{Li}^+(TP)−V_{Li}^- (Oct)	1.22	6×10^{2}
Co_{Li}^+(TP)−V_{Li}^- (TP)	1.45	9×10^{-2}
Co_{Li}^{2+}(Oct)−V_{Li}^- (Oct)	2.57	2×10^{-20}
Co_{Li}^{2+}(Oct)−V_{Li}^- (TP)	2.45	1×10^{-18}
Co_{Li}^{2+}(TP)−V_{Li}^- (Oct)	2.65	7×10^{-22}
Co_{Li}^{2+}(TP)−V_{Li}^- (TP)	4.02	7×10^{-45}

over the TP site. The lowest-energy configuration under equilibrium conditions is the Co_{Li}^+(Oct)−V_{Li}^-(TP) complex, with a formation energy of 0.30 eV, representing a 13 ppm doping level (2×10^{18} cm^{-3}). Since this complex is electrically neutral, it will not affect the Fermi level. The lowest-energy charged substitution is Co_{Li}^+(Oct), which corresponds to the substitution of a Li^+ ion with a Co^{2+} ion. The calculated equilibrium formation energy of Co_{Li}^+(Oct) is 0.36 eV, which corresponds to a 1 ppm doping level (7×10^{16} cm^{-3}). To put this in context, note that the calculated Co concentration is comparable to the level of inorganic ionic impurities typically incorporated during electrodeposition of metals (10^{-5}–10^{-4} atomic fraction[32]) and is also within the typical range of dopant concentrations in semiconductor devices (10^{-8}–10^{-5} atomic fraction[57]). Notably, the Co_{Li}^+(Oct) defect has a significantly lower formation energy than the hole polaron (the dominant positive intrinsic defect). Thus, the introduction of Co could cause a substantial change in the defect chemistry, since the Fermi level relative to the local electrostatic potential is shifted to higher energies. Consequently, in the presence of Co dopants the concentration of V_{Li}^- increases 9 orders of magnitude to 7×10^{16} cm^{-3} (i.e., Li^+ ions are removed to compensate for the charge of the Co_{Li}^+), and the concentration of p^+ decreases to 1×10^{-3} cm^{-3}. For comparison, the equilibrium concentrations of p^+ and V_{Li}^- in the absence of dopants are of the order of 10^7 cm^{-3}.[28]

One factor contributing to the stability of the Co substitutions may be the minimal strain they exert on the Li_2O_2 lattice: the relaxation of the Co_{Li}^+(Oct) geometry results in only a 2% change in the cation−anion nearest neighbor distance. Other factors appear to be significant as well, however. For example, Co_{Li}^+ is about 1 eV higher in energy at the TP site than the Oct site, despite having a similar lattice strain energy (see Supporting Information for details). The differing stabilities of these two sites can be attributed to differences in crystal field stabilization energy, as discussed in more detail in the Supporting Information.

3. TRANSPORT MODEL

Having established the concentration of Co dopants in Li_2O_2 at equilibrium, it becomes possible to examine the effect that this doping exerts on transport within the Li_2O_2 discharge phase. To this end, a one-dimensional transport model based on Nernst−Planck theory was developed to calculate the quasi-steady-state voltage drop associated with charge transport through doped Li_2O_2. This voltage drop represents the contribution of charge-transport limitations to the cell's overpotential. In the present context, "quasi-steady-state" is intended to mean that diffusional relaxations associated with local accumulation of material occur very rapidly in comparison to the time scale of interest, and also that the film thickness changes sufficiently slowly on this time scale that the velocity of the peroxide film's boundaries can be neglected. The former is valid when the characteristic diffusion time for the slowest-diffusing species is much shorter than the period of discharge or charge; indeed this is the case for hole polarons and Li-ion vacancies under realistic operating conditions.[28]

Figure 2 illustrates two scenarios, motivated by previous experimental and theoretical studies, to which the transport

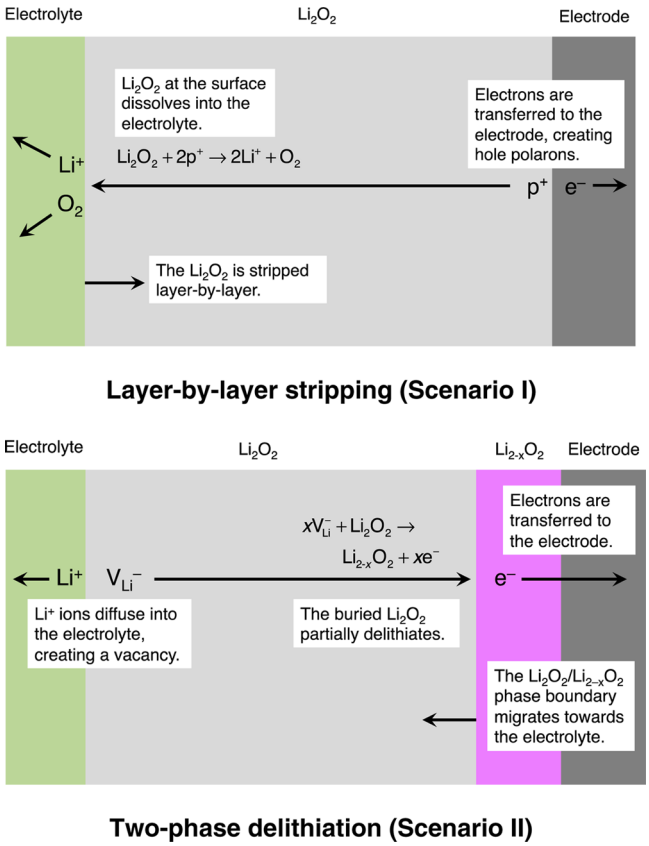

Figure 2. Model for transport through a doped Li_2O_2 film during recharge in the case of (top) Scenario I: layer-by-layer stripping and (bottom) Scenario II: two-phase delithiation. Here p^+ refers to a hole polaron in Li_2O_2, which moves in the opposite direction as an electron, e^-. Similarly, V_{Li}^- refers to a negatively charged Li vacancy, which moves in the opposite direction as a Li^+ ion.

model is applied: (a) the layer-by-layer electrochemical deposition/stripping of the Li_2O_2 deposit, occurring at the Li_2O_2/electrolyte interface,[30] and (b) a two-phase delithiation mechanism, in which delithiation of Li_2O_2 starts at the buried Li_2O_2/electrode interface and Li^+ diffuses through the film to reach the electrolyte.[28,58,59] Key differences between the scenarios are summarized below:

1. While Scenario I (layer-by-layer stripping/deposition) can represent mechanisms for both discharge and charge,

DOI: 10.1021/cm503874c
Chem. Mater. 2015, 27, 839−847

Scenario II (two-phase delithiation) applies only to charging.

2. As is shown below, steady-state charge transport through Li_2O_2 in Scenario I is mediated by hole polarons; in Scenario II, Li-ion vacancies mediate charge transport. Both mechanisms are illustrated qualitatively in Figure 2.
3. The overall half-reaction for oxidation in Scenario I is $1/2Li_2O_2(p) \rightarrow Li^+(l) + 1/2O_2(l) + e^-(s)$ [where (p) indicates a species in the discharge-product phase, (l) a species in the liquid−electrolyte phase, and (s) a species in the Li/O_2 electrode's support material], but in Scenario II it is $Li_2O_2(p) \rightarrow xLi^+(l) + Li_{2-x}O_2(p) + xe^-(s)$. Presumably, the oxidation of Li_2O_2 to $Li_{2-x}O_2$ in Scenario II would be followed by a subsequent oxidation of $Li_{2-x}O_2$ to form molecular O_2.

Scenario I assumes that the accumulation of defects does not produce a distinct solid phase within the peroxide film. (In principle, the accumulation of V_{Li}^- and p^+ could lead to the nucleation of a lithium-deficient $Li_{2-x}O_2$ phase; Scenario II describes one such situation.) The defect concentration in Scenario I is small enough (~1 ppm, as shown below) that the nucleation of a Li-deficient phase may not occur. Also, observe that an accumulation of both lithium and oxygen vacancies could lead to void formation, but the high barrier for oxygen-vacancy diffusion in Li_2O_2 (1.5 eV)[60] suggests that voids are unlikely.

Scenario II is motivated by a recent study which predicted that Li_2O_2 could be topotactically delithiated via a two-phase pathway to lithium superoxide (LiO_2) at moderate charge potentials (3.3−3.4 V vs Li/Li^+).[59] The presence of a plateau at 3.4−3.5 V vs Li/Li^+ during potentiostatic intermittent titration technique (PITT) experiments on Li/O_2 cells also supports a two-phase delithiation hypothesis.[61,62] The formation of LiO_2 corresponds to $x = 1$, although other Li-deficient stoichiometries may be possible; it has been suggested that a $Li_{2-x}O_2$ ($0 < x < 1$) solid solution may form.[28] Electron-transport limitations through a Li-deficient phase could also contribute to charging overpotentials, but any such limitations are neglected here because (i) the high electronic conductivity reported for crystalline KO_2 suggests that other superoxide phases such as LiO_2 may also have a high electronic conductivity,[63] and (ii) a $Li_{2-x}O_2$ ($0 < x < 1$) solid-solution phase is expected to have a high electronic conductivity associated with electron hopping.[28]

Prior studies have treated transport in Li_2O_2 through simplified models wherein the carrier concentrations are taken to be spatially and temporally uniform.[28,30,58] Although these studies provide important baselines, the incorporation of concentration gradients within the present model leads to qualitatively different, and presumably more accurate, current−voltage relationships for transport through doped Li_2O_2. The model described below indicates that charge transport through doped Li_2O_2 is facile in both scenarios during recharge.

Governing Equations. The model accounts for four mobile species in the Li_2O_2 film: V_{Li}^-, p^+, Co_{Li}^+, and $V_{Li}^- - Co_{Li}^+$ bound pairs. The most fundamental model equations describe the continuity of material, which requires that (i) the fluxes of Li and Co atoms are divergence free,

$$\frac{d}{dy}(N_{V_{Li}^-} + N_{Co_{Li}^+ - V_{Li}^-}) = 0 \quad \text{and} \quad \frac{d}{dy}(N_{Co_{Li}^+} + N_{Co_{Li}^+ - V_{Li}^-}) = 0 \tag{2}$$

where N_k is the flux of species k, and (ii) the continuity of charge, which requires that the current density i also be divergence free,

$$\frac{di}{dy} = 0 \tag{3}$$

In addition to obeying a continuity equation, charge is taken to balance locally through the electroneutrality constraint

$$c_{p^+} - c_{V_{Li}^-} + c_{Co_{Li}^+} = 0 \tag{4}$$

where c_k represents the number density of species k. This approximation is suitable for a doped film under typical operating conditions for a Li/O_2 electrode, except in certain regimes where double-layer charging becomes important, as discussed below and in the Supporting Information.

Constitutive Laws. Inside the Li_2O_2 film Nernst−Planck flux laws describe the diffusion and migration of each species k,

$$N_k = -D_k\frac{dc_k}{dy} - \frac{D_k z_k e}{k_B T}c_k\frac{d\Phi}{dy} \tag{5}$$

where Φ is the electrostatic potential, k_B is the Boltzmann constant, e is the elementary charge, and $T = 300$ K is the absolute temperature; D_k represents the diffusivity of species k and z_k its equivalent charge ($z_{V_{Li}^-} = -1$, $z_{p^+} = +1$, $z_{Co_{Li}^+} = +1$, and $z_{Co_{Li}^+ - V_{Li}^-} = 0$). Note that Nernst−Planck theory only applies to point defects if their concentrations are relatively low;[64] this approximation is fair under operating regimes relevant for Li/O_2 batteries. Charge flux follows from the material fluxes through Faraday's law,

$$i = e(N_{p^+} - N_{V_{Li}^-} + N_{Co_{Li}^+}) \tag{6}$$

Here i is defined as a cathodic current, meaning that $i > 0$ for discharge and $i < 0$ for recharge. The diffusion coefficients of hole polarons and Li-ion vacancies were taken from our prior DFT calculations ($D_{p^+} = 9 \times 10^{-10}$ cm^{2}s^{-1} and $D_{V_{Li}^-} = 6 \times 10^{-9}$ cm^{2}s^{-1}).[28] Co is assumed to diffuse via a vacancy-mediated mechanism as a $V_{Li}^- - Co_{Li}^+$ bound pair, and the contributions of other diffusion mechanisms are neglected. Consequently, the mobility of unbound Co is negligible ($D_{Co_{Li}^+} \approx 0$), causing the unbound-Co flux to vanish everywhere. As shown below, no assumptions about the value of the bound-pair diffusivity need be made, since the net flux of bound pairs vanishes uniformly; this also implies that bound-pair diffusion does not affect the potential drop.

Vacancy-substitution association/dissociation ($Co_{Li}^+ + V_{Li}^- \leftrightarrow Co_{Li}^+ - V_{Li}^-$) is taken to be in local equilibrium,

$$\frac{c_{V_{Li}^-}c_{Co_{Li}^+}}{c_{Co_{Li}^+ - V_{Li}^-}} = \frac{c^0_{V_{Li}^-}c^0_{Co_{Li}^+}}{c^0_{Co_{Li}^+ - V_{Li}^-}} \tag{7}$$

Thus, the reaction quotient for defect dissociation remains constant and is determined by parameters from Table 1.

Boundary Conditions. The film is taken to be planar and one-dimensional, with y representing the direction normal to the interfaces with the electrode and electrolyte. Boundary conditions differ for Scenario I (layer-by-layer deposition/stripping) and Scenario II (two-phase delithiation). In both scenarios we require defect formation to be in equilibrium with O_2, Li_2O_2, and $LiCoO_2$ at the Li_2O_2/electrolyte interface, corresponding to position $y = 0$. This constrains the concentrations of defects to those shown in Table 1:

$$c_i(0) = c_i^0 \tag{8}$$

These constraints combine with the defect-dissociation equilibrium described by eq 7 to show that the concentration of

DOI: 10.1021/cm503874c
Chem. Mater. 2015, 27, 839−847

$Co_{Li}^{+}-V_{Li}^{-}$ bound pairs at the Li_2O_2/electrolyte interface is also fixed.

The boundary at $y = L$ represents the Li_2O_2/electrode interface in Scenario I and the $Li_2O_2/Li_{2-x}O_2$ interface in Scenario II. Both scenarios require that the flux of Co through the $y = L$ boundary be zero because the electrode is assumed to block flux of ionic Co:

$$N_{Co_{Li}^{+}}(L) + N_{Co_{Li}^{+}-V_{Li}^{-}}(L) = 0. \quad (9)$$

In Scenario I, there exists the additional stipulation that the flux of Li vacancies across the Li_2O_2/electrode interface should vanish, since the electrode blocks Li-ion transport:

$$N_{V_{Li}^{-}}(L) + N_{Co_{Li}^{+}-V_{Li}^{-}}(L) = 0. \quad (10)$$

In Scenario II, polarons are not consumed or produced at the Li_2O_2/electrolyte interface (or at least the rate of polaron consumption/production is assumed to be negligible compared to the rate of delithiation). Thus, the flux of hole polarons across the Li_2O_2/electrolyte interface is zero in Scenario II:

$$N_{p^{+}}(0) = 0 \quad (11)$$

General Remarks. Important consequences of the model assumptions laid out above include the following:

1. By combining the material balances from eq 2, the ion-blocking condition on Co from eq 9, and the fact that the flux of Co_{Li}^{+} vanishes, the steady-state flux of $Co_{Li}^{+}-V_{Li}^{-}$ bound pairs vanishes everywhere: $N_{Co_{Li}^{+}-V_{Li}^{-}}(y) = 0$.
2. Since $N_{Co_{Li}^{+}-V_{Li}^{-}}(y) = 0$ and bound pairs are electrically neutral, the flux law from eq 5 requires the number density $c_{Co_{Li}^{+}-V_{Li}^{-}}$ to be uniform throughout the film.
3. Because the concentration of bound pairs is uniform, the defect association/dissociation equilibrium, eq 7, requires that gradients in the V_{Li}^{-} and Co_{Li}^{+} concentrations are always opposed (i.e., $dc_{V_{Li}^{-}}/dy$ and $dc_{Co_{Li}^{+}}/dy$ have opposing signs).
4. To maintain the electroneutrality condition from eq 4, gradients in the V_{Li}^{-} and p^{+} concentrations have coincident directions (i.e., $dc_{V_{Li}^{-}}/dy$ and $dc_{p^{+}}/dy$ have similar signs).

Before discussing the predictions of the transport model, it is first worth commenting on its connection to the equilibrium concentrations derived from Figure 1. As previously mentioned, the concentrations c_k^0 establish a boundary condition at the Li_2O_2/electrolyte interface ($y = 0$), where equilibrium with O_2, Li_2O_2, and $LiCoO_2$ is assumed to hold. Solving the transport model then yields species number densities as functions of position; the $c_k(y)$ vary spatially due to changes in local electrochemical potentials. Thus, a solution to the transport model is akin to generating a formation-energy diagram (with a unique Fermi level) at each point y in the film based on values of the electrochemical potentials there.

Scenario I: Layer-by-Layer Stripping/Deposition. By combining material continuity with the ion-blocking condition on Li, and the fact that the bound-pair flux uniformly vanishes, it follows that the flux of Li-ion vacancies vanishes uniformly: $N_{V_{Li}^{-}}(y) = 0$. Thus, all of the current is carried by hole polarons, as indicated in Figure 2. From the above equations, the current through a film of thickness L is shown to be

$$i = \frac{2eD_{p^{+}}c_{V_{Li}^{-}}^{0}}{L}\left[1 - \exp\left(\frac{e\Delta\Phi}{k_B T}\right)\right] \quad (12)$$

(Note that the diffusion coefficients of bound pairs and lithium vacancies do not appear here, because the net fluxes of these species vanish, as discussed above.) Equation 12 predicts that the peroxide film acts like a diode: the negative current responds exponentially, allowing arbitrarily large anodic (recharge) currents ($i < 0$), whereas the cathodic (discharge) current ($i > 0$) saturates when $|\Delta\Phi| \gg k_B T/e$. Equation 12 suggests a limiting cathodic current density of $2eD_{p^{+}}c_{V_{Li}^{-}}^{0}$. As discussed in the Supporting Information, however, electroneutrality does not hold in the positive current (discharge) regime of Scenario I because the Li_2O_2/electrode interface becomes starved of polarons and the charging of the double-layer at that interface accommodates most of the potential drop. In the Supporting Information, we modify the model to account for electroneutrality violations and show that the discharge current indeed does saturate but not at the value implied by eq 12. An upper bound on the cathodic current density is shown to be approximately $eD_{p^{+}}c_{p^{+}}^{0}/L$, which for a 100 nm thick film corresponds to $\sim 10^{-20}$ μA/cm^2. This current is far smaller than experimentally observed current densities during discharge.

Although only minimal discharge currents can be supported, recharge is predicted to be quite facile. Figure 3 shows the potential drop calculated from eq 12 as a function of anodic (recharge) current for various film thicknesses. The potential drop needed to drive recharge is quite small in the presence of Co dopants. For example, a potential drop of only 10 mV is needed to drive a current density of 1 μA/cm^2 through a 100 nm thick film. This current density is fairly representative of the microscopic current densities of typical Li/O_2 experiments[61,65] and would correspond to a 27-h charge for a 100 nm thick film. (1 μA/cm^2 also is representative of the estimated microscopic current density required to achieve the macroscopic current density target described in the literature.[28,66]) This result contrasts strongly with undoped Li_2O_2, whose low intrinsic conductivity is thought to be a performance-limiting factor.[28−30] Thus, our results indicate that donor doping, such as through the incorporation of Co substitutions, can in principle moderate charge transport limitations in the Li/O_2 discharge product during recharge.

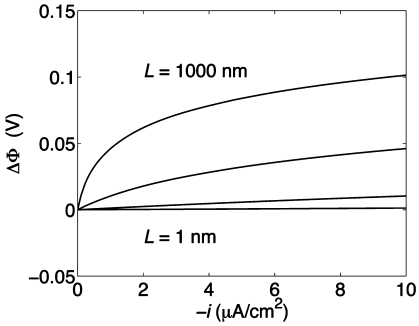

Figure 3. Calculated potential drop during recharge as a function of current density across doped Li_2O_2 films of thickness 1, 10, 100, and 1000 nm in Scenario I (layer-by-layer stripping/deposition).

Figure 4 shows the steady-state concentrations of defects and the electrostatic potential across the film for 1 μA/cm^2 charging of a 100 nm thick film. At the Li_2O_2/electrolyte interface ($y = 0$), the addition of dopants lowers the number density of p^{+} and increases that of V_{Li}^{-} as the Fermi level shifts to higher energies (cf. Figure 1 and eqs 4 and 7). As discussed above, the

DOI: 10.1021/cm503874c
Chem. Mater. 2015, 27, 839−847

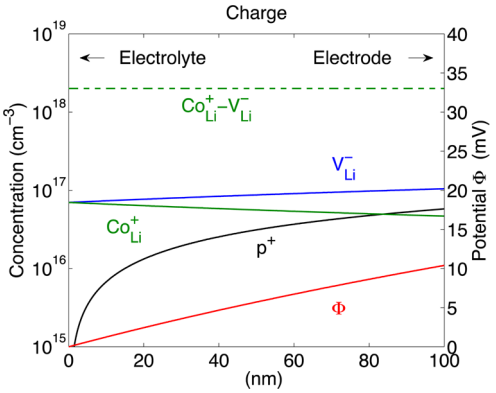

Figure 4. Calculated defect concentrations and electrostatic potential for Scenario I (layer-by-layer stripping/deposition) in a 100 nm doped Li_2O_2 film during charge at a current density of 1 μA/cm^2.

net V^-_{Li} flux must vanish. Thus, the electrostatic force pushing lithium vacancies toward the electrode, a consequence of the rise in potential as y increases, must be balanced by an opposing flux arising from a concentration gradient. Consequently, the concentration of V^-_{Li} rises as one approaches the electrode (increasing y) in Figure 4.

This gradient in the V^-_{Li} concentration is accompanied by a gradient in the p^+ concentration with the same sign, as discussed above. As more Co is added to the film, the number density of V^-_{Li} at the Li_2O_2/electrolyte interface rises, and a larger gradient of V^-_{Li} concentration is needed to compensate for the electric field. Consequently, increased doping leads to a larger p^+ concentration gradient. In a highly doped sample, the p^+ concentration will rapidly rise as one moves away from the Li_2O_2/electrolyte interface, resulting in an increased electronic film conductance during recharge.

The conclusion that Co substitutions should enhance charge transport during recharge may appear counterintuitive, given that the addition of Co donors shifts the equilibrium Fermi level toward higher energies (Figure 1), thereby reducing the equilibrium polaron concentration. The present model reveals that this effect, which applies only as an equilibrium boundary condition at the Li_2O_2/electrolyte interface, is in fact offset by the conductivity enhancement associated with the accumulation of V^-_{Li} and p^+ deeper into the film. The accumulation of V^-_{Li} and p^+ represents a partial delithiation of the discharge product. Unlike Scenario II, however, this delithiation represents a concentration gradient of vacancies, rather than the formation of a new lithium-deficient phase.

Scenario II: Two-Phase Delithiation. In the case of a delithiation recharge mechanism, one can combine continuity of mass and charge (eqs 2 and 3), Faraday's law (eq 6), and the boundary condition on hole polaron flux (eq 11) to show that the flux of hole polarons vanishes everywhere. Thus, all of the current is carried by Li-ion vacancies, consistent with the schematic in Figure 2. The model's behavior is straightforward in the limit that the dopant concentration is much larger than the intrinsic defect concentration in the absence of impurities. It can be shown that the concentration of vacancies in this limit is uniform throughout the film, and the current−voltage relationship is Ohmic,

$$i = -\frac{e^2 D_{V^-_{Li}} c^0_{V^-_{Li}} \Delta\Phi}{k_B T L} \tag{13}$$

The effective conductivity $e^2 D_{V^-_{Li}} c^0_{V^-_{Li}}/k_B T$ is 3×10^{-9} S/cm. This is 9 orders of magnitude larger than the predicted intrinsic ionic conductivity of crystalline Li_2O_2[28] and is high enough to provide adequate charge transport under typical conditions in a Li/O_2 cell. For example, a 1 μA/cm^2 current through a 100 nm thick film results in a potential drop of only 4 mV.

4. DISCUSSION

The multiscale model predicts that doped Li_2O_2 cannot support appreciable currents during discharge due to the limited charge transport supported by hole polarons, as shown in eq 12. (The contribution of lithium vacancies to conductivity is also limited, as it has been assumed that the electrode blocks their transport during discharge.) The fact that large Li_2O_2 deposits are nevertheless observed in Li/O_2 cells suggests that either[28] (i) alternative electronic charge transport pathways exist (e.g., surfaces[28] or grain boundaries[67]), or (ii) particle growth can occur via the solution-mediated transport and subsequent precipitation of a soluble species[12] (e.g., LiO_2). The fact that very similar biconcave disk morphologies have been observed in the chemical deposition of unrelated systems supports the latter explanation.[68,69]

On the other hand, the model indicates that during recharge, charge transport in doped Li_2O_2 is facile, regardless of whether the OER occurs via layer-by-layer stripping (Scenario I) or two-phase delithiation (Scenario II). This suggests that the doping of the discharge product may be a promising strategy for overcoming high charging overpotentials in Li/O_2 batteries. We speculate that the improved transport properties of doped Li_2O_2 may explain the reduced charging overpotentials observed in recent experiments on Co_3O_4-based electrodes.[9] Our proposed mechanism is illustrated in Figure 5. First, a small amount of Co dissolves into the electrolyte. Next, the solvated Co ions are incorporated into the discharge product. Finally, the presence of Co dopants in the discharge product enhances charge transport during recharge, and the OER proceeds via either layer-by-layer stripping or two-phase delithiation. Although we have presented this mechanism as a three-step process, some or all of these steps may occur simultaneously. Additionally, solid-state diffusion of Co (not shown) represents another possible route for Co incorporation.

The doping of Li/O_2 discharge products is unlike the ex situ doping of conventional semiconducting materials or Li-ion battery materials (e.g., $LiFePO_4$[70,71]). In Li/O_2 cells the discharge product is in principle deposited and dissolved at every cycle. Therefore, any successful doping strategy must occur in situ during each charge/discharge cycle and at a sufficient concentration. Black et al.[9] found that the ability of Co_3O_4 to promote the OER was reproducible over many cycles, suggesting that if Co doping was indeed responsible for this behavior, then the incorporation of Co occurred repeatedly.

Of course the relative importance of different discharge/recharge mechanisms may also be influenced by experimental details such as electrode support material, depth of discharge, system cleanliness, etc. These factors are not included in the present model. For example, several studies have suggested that when the discharge product is a thin film (~4 nm or less), charge transport through Li_2O_2 occurs via electron tunneling.[30,65,72] The present model is intended to capture transport through thicker deposits (10−1000 nm), which would be desirable for achieving high capacities. In such cases electron tunneling is thought to be negligible. Further discussion regarding electron tunneling and methodological differences

DOI: 10.1021/cm503874c
Chem. Mater. 2015, 27, 839−847

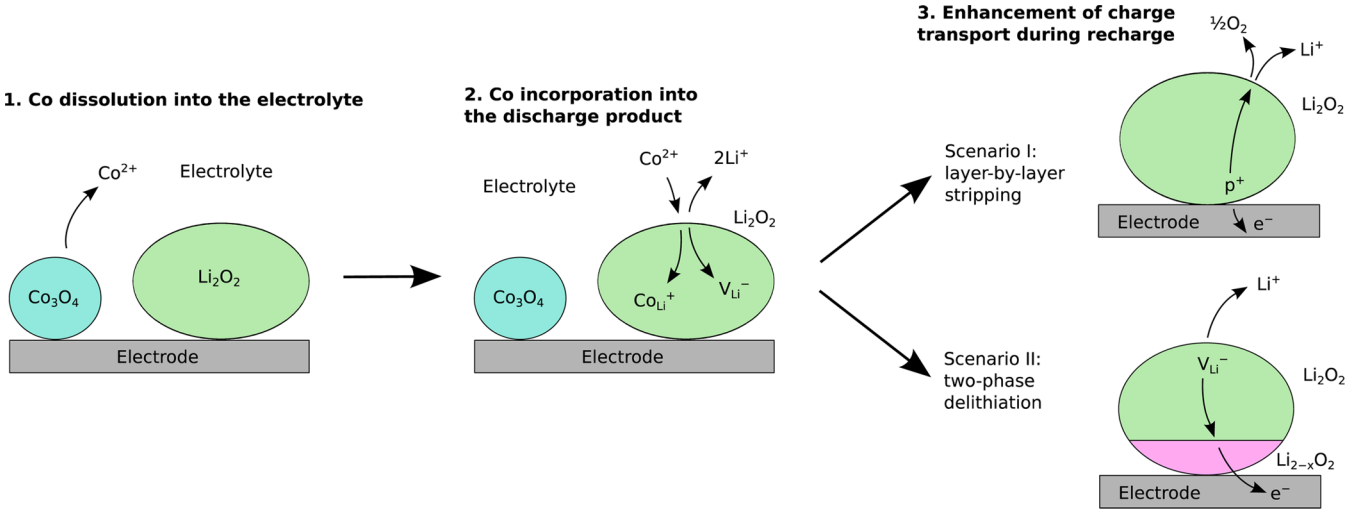

Figure 5. Proposed mechanism for the promotion of the OER in Co_3O_4-containing electrodes. For simplicity, dissolved Co ions are assumed to have a 2+ charge.

between our work and that of Varley et al.[72] is provided in the Supporting Information.

To explore the possibility that other elements could dope Li_2O_2, formation energies for extrinsic defects involving 22 other elements were calculated, as shown in the Supporting Information, Figure S6. Nickel, like Co, is predicted to significantly shift the Fermi level relative to its position in undoped Li_2O_2 (Figure S7, Supporting Information). We therefore speculate that Ni-containing compounds could also promote recharge in Li/O_2 cells; this hypothesis is supported by the observed lowering of charge overpotentials in Li/O_2 cells containing NiO[20,73] and $NiCo_2O_4$.[24] Of the remaining elements, none are predicted to shift the Fermi level as significantly as Co and Ni, as shown in Figure S7 and Table S5, Supporting Information. Some of the other transition metals, notably Pt and Ru, as well as non-transition metals and halogens are predicted to have formation energies similar to that of the intrinsic defects. On the other hand, essentially all of the pnictogens and metalloids investigated have formation energies significantly higher than that of the intrinsic defects.

The mechanism for OER promotion hypothesized in the present study should also be considered in light of the lowered charging potentials observed in cells *preloaded* with Li_2O_2 in the presence of Pt, Ru, Au, or various transition metal oxides additions.[7,8,20,37] In these cases ex situ sonication or stirring was used[7,8] and may have driven dopant incorporation above the equilibrium levels considered in the present study; therefore, a direct comparison with computational predictions may not be justified. Nevertheless, it is noteworthy that the trend in the calculated formation energies for Pt, Ru, and Au dopants (Figure S7) correlates with the trend in OER activity reported by Harding et al.,[7] who observed that the charging overpotentials of cells preloaded with Li_2O_2 were reduced by the addition of Pt and Ru but not Au. On the other hand, there is little correlation between the calculated defect formation energies and the trend in OER activities observed by Giordani et al.[20] for electrodes preloaded with mixtures of Li_2O_2 and various transition metal oxides. For example, NiO was observed to have very little effect on charging overpotentials compared to MnO_2; in contrast, our calculations predict Ni substitutions in Li_2O_2 to be much more favorable than Mn substitutions. Thus, if doping is responsible for reduced overpotentials in this experiment, then factors beyond the equilibrium defect formation energy presumably must play a role in determining the relative efficacy of these promoters. For example, the incorporation of dopants into the interior of the Li_2O_2 particles during the mixing process may have been incomplete.

Finally, the enhancement of charge transport predicted by the model developed here differs from the "polaron preemption" mechanism recently hypothesized for Li_2O_2 that is highly doped (~2%) with silicon.[27] The polaron preemption mechanism involves a change to the host's electronic structure, driven by a high level of impurities. In contrast, the present mechanism involves a change in the dynamic equilibrium between vacancies and polarons due to the introduction of trace (ppm-level) impurities.

5. CONCLUSION

Understanding of the mechanism by which promoters enhance the oxygen evolution reaction is an important step in the rational design of Li/O_2 electrode materials. Here a multiscale model has been developed that can explain the ability of Co_3O_4 to promote oxidation of bulk Li_2O_2 and consequently improve the voltaic efficiency of Li/O_2 batteries.[7−9,37] The promotion effect is hypothesized to arise from enhanced electronic and/or ionic transport within the discharge product due to in situ doping of the Li_2O_2 discharge phase with Co. This hypothesis is supported by calculations, which show that thick Li_2O_2 deposits doped with Co can support large recharge current densities with only minimal overpotentials. In particular, a Li_2O_2 film doped at low ppm levels will have an effective conductivity of 10^{-9} S/cm or higher during recharge, regardless of whether decomposition occurs via layer-by-layer stripping or two-phase delithiation. Under typical experimental conditions, a conductivity of this magnitude would reduce contributions to the overpotential from charge-transport limitations to the order of millivolts. Although the proposed mechanism is not "catalytic" in the traditional sense, it may provide insight into the effect (or non-effect) of various putative catalysts on the Li/O_2 OER. On the basis of a computational assessment of 22 additional dopants, we speculate that Ni may also be an effective OER promoter. Quantifying the Co or Ni content of the discharge product could test the hypothesis that doping is responsible for the promotion of the OER. However, the detection of ppm

DOI: 10.1021/cm503874c
Chem. Mater. 2015, 27, 839−847

levels of doping may be difficult. Lastly, we speculate that adding Co or Ni salts to the electrolyte could also facilitate the doping of the discharge product and therefore promote the OER.

■ ASSOCIATED CONTENT

Supporting Information

Details of point defect calculations, non-electroneutral transport model, additional discussion of relevant literature, and formation energies of other extrinsic defects. This material is available free of charge via the Internet at http://pubs.acs.org.

■ AUTHOR INFORMATION

Corresponding Author

*E-mail: djsiege@umich.edu.

Notes

The authors declare no competing financial interest.

■ ACKNOWLEDGMENTS

This work was supported by Robert Bosch LLC through the Bosch Energy Research Network, grant no. 19.04.US11, and by the U.S. National Science Foundation, grant no. CBET-1336387.

■ REFERENCES

(1) Hardwick, L. J.; Bruce, P. G. *Curr. Opin. Solid State Mater. Sci.* **2012**, *16*, 178−185.
(2) Christensen, J.; Albertus, P.; Sánchez-Carrera, R. S.; Lohmann, T.; Kozinsky, B.; Liedtke, R.; Ahmed, J.; Kojic, A. *J. Electrochem. Soc.* **2012**, *159*, R1−R30.
(3) Lu, Y.-C.; Gallant, B. M.; Kwabi, D. G.; Harding, J. R.; Mitchell, R. R.; Whittingham, M. S.; Shao-Horn, Y. *Energy Environ. Sci.* **2013**, *6*, 750.
(4) Garcia-Araez, N.; Novák, P. *J. Solid State Electrochem.* **2013**, *17*, 1793−1807.
(5) McCloskey, B.; Scheffler, R.; Speidel, A.; Bethune, D. S.; Shelby, R. M.; Luntz, A. C. *J. Am. Chem. Soc.* **2011**, *133*, 18038−18041.
(6) Li, F.; Zhang, T.; Zhou, H. *Energy Environ. Sci.* **2013**, *6*, 1125−1141.
(7) Harding, J. R.; Lu, Y.; Shao-horn, Y. *Phys. Chem. Chem. Phys.* **2012**, *14*, 10540−10546.
(8) Meini, S.; Tsiouvaras, N.; Schwenke, K. U.; Piana, M.; Beyer, H.; Lange, L.; Gasteiger, H. a. *Phys. Chem. Chem. Phys.* **2013**, *15*, 11478−11493.
(9) Black, R.; Lee, J.-H.; Adams, B.; Mims, C. a; Nazar, L. F. *Angew. Chem., Int. Ed.* **2013**, *52*, 392−396.
(10) Shao, Y.; Ding, F.; Xiao, J.; Zhang, J.; Xu, W.; Park, S.; Zhang, J.-G.; Wang, Y.; Liu, J. *Adv. Funct. Mater.* **2013**, *23*, 987−1004.
(11) Viswanathan, V.; Nørskov, J. K.; Speidel, A.; Scheffler, R.; Gowda, S.; Luntz, A. C. *J. Phys. Chem. Lett.* **2013**, *4*, 556−560.
(12) Adams, B. D.; Radtke, C.; Black, R.; Trudeau, M. L.; Zaghib, K.; Nazar, L. F. *Energy Environ. Sci.* **2013**, *6*, 1772.
(13) Oh, S.; Black, R.; Pomerantseva, E.; Lee, J.; Nazar, L. *Nat. Chem.* **2012**, *4*, 1004−1010.
(14) Lu, J.; Lei, Y.; Lau, K. C.; Luo, X.; Du, P.; Wen, J.; Assary, R. S.; Das, U.; Miller, D. J.; Elam, J. W.; Albishri, H. M.; El-Hady, D. A.; Sun, Y.-K.; Curtiss, L. a.; Amine, K. *Nat. Commun.* **2013**, *4*, 2383.
(15) Xu, J.-J.; Wang, Z.-L.; Xu, D.; Zhang, L.-L.; Zhang, X.-B. *Nat. Commun.* **2013**, *4*, 2438.
(16) Yilmaz, E.; Yogi, C.; Yamanaka, K.; Ohta, T.; Byon, H. R. *Nano Lett.* **2013**, *13*, 4679−4684.
(17) Xia, C.; Waletzko, M.; Peppler, K.; Janek, J. *J. Phys. Chem. C* **2013**, *117*, 19897−19904.
(18) Cui, Y.; Wen, Z.; Sun, S.; Lu, Y.; Jin, J. *Solid State Ionics* **2012**, *225*, 598−603.
(19) Riaz, A.; Jung, K.-N.; Chang, W.; Lee, S.-B.; Lim, T.-H.; Park, S.-J.; Song, R.-H.; Yoon, S.; Shin, K.-H.; Lee, J.-W. *Chem. Commun. (Cambridge, U. K.)* **2013**, *49*, 5984−5986.
(20) Giordani, V.; Freunberger, S. A.; Bruce, P. G.; Tarascon, J.-M.; Larcher, D. *Electrochem. Solid-State Lett.* **2010**, *13*, A180.
(21) Ryu, W.; Yoon, T.; Song, S. H.; Jeon, S.; Park, Y.; Kim, I. *Nano Lett.* **2013**, *13*, 4190−4197.
(22) Cui, Y.; Wen, Z.; Liu, Y. *Energy Environ. Sci.* **2011**, *4*, 4727−4734.
(23) Zhang, K.; Zhang, L.; Chen, X.; He, X.; Wang, X.; Dong, S.; Han, P.; Zhang, C.; Wang, S.; Gu, L.; Cui, G. *J. Phys. Chem. C* **2013**, *117*, 858−865.
(24) Sun, B.; Zhang, J.; Munroe, P.; Ahn, H.-J.; Wang, G. *Electrochem. Commun.* **2013**, *31*, 88−91.
(25) Trahey, L.; Karan, N. K.; Chan, M. K. Y.; Lu, J.; Ren, Y.; Greeley, J.; Balasubramanian, M.; Burrell, A. K.; Curtiss, L. a.; Thackeray, M. M. *Adv. Energy Mater.* **2012**, *3*, 75−84.
(26) Thackeray, M. M.; Chan, M. K. Y.; Trahey, L.; Kirklin, S.; Wolverton, C. *J. Phys. Chem. Lett.* **2013**, *4*, 3607−3611.
(27) Timoshevskii, V.; Feng, Z.; Bevan, K. H.; Goodenough, J.; Zaghib, K. *Appl. Phys. Lett.* **2013**, *103*, 073901.
(28) Radin, M. D.; Siegel, D. J. *Energy Environ. Sci.* **2013**, *6*, 2370−2379.
(29) Gerbig, O.; Merkle, R.; Maier, J. *Adv. Mater.* **2013**, *25*, 3129−3133.
(30) Luntz, A. C.; Viswanathan, V.; Voss, J.; Varley, J. B.; Speidel, A. *J. Phys. Chem. Lett.* **2013**, *4*, 3494−34997.
(31) Amatucci, G. G.; Tarascon, J. M.; Klein, L. C. *Solid State Ionics* **1996**, *83*, 167−173.
(32) Gamburg, Y. D.; Zangari, G. *Theory and Practice of Metal Electrodeposition*; Springer Science+Business Media, LLC: New York, 2011.
(33) Zhang, S. S. *J. Power Sources* **2006**, *162*, 1379−1394.
(34) Veith, G. M.; Nanda, J.; Delmau, L. H.; Dudney, N. J. *J. Phys. Chem. Lett.* **2012**, *3*, 1242−1247.
(35) Tilley, R. J. D. *Defects in Solids*; John Wiley & Sons, Inc.: Hoboken, NJ, 2008.
(36) Kröger, F. A. *The chemistry of imperfect crystals*; North-Holland Pub. Co.; American Elsevier: Amsterdam, 1973.
(37) Sun, B.; Munroe, P.; Wang, G. *Sci. Rep.* **2013**, *3*, 2247.
(38) Königstein, M. *J. Solid State Chem.* **1999**, *147*, 478−484.
(39) Roth, R. S.; Rawn, C. J.; Hill, M. D. *NIST Spec. Publ.* **1991**, *804*, 225−236.
(40) Ong, S. P.; Mo, Y.; Ceder, G. *Phys. Rev. B* **2012**, *85*, 081105.
(41) Kang, J.; Jung, Y. S.; Wei, S.-H.; Dillon, A. *Phys. Rev. B* **2012**, *85*, 035210.
(42) Garcia-Lastra, J. M.; Myrdal, J. S. G.; Christensen, R.; Thygesen, K. S.; Vegge, T. *J. Phys. Chem. C* **2013**, *117*, 5568−5577.
(43) Van de Walle, C. G.; Neugebauer, J. *J. Appl. Phys.* **2004**, *95*, 3851.
(44) Heyd, J.; Scuseria, G. E.; Ernzerhof, M. *J. Chem. Phys.* **2003**, *118*, 8207.
(45) Krukau, A. V.; Vydrov, O. a.; Izmaylov, A. F.; Scuseria, G. E. *J. Chem. Phys.* **2006**, *125*, 224106.
(46) Kresse, G.; Hafner, J. *Phys. Rev. B* **1994**, *49*, 14251−14269.
(47) Kresse, G.; Furthmüller, J. *Phys. Rev. B* **1996**, *54*, 11169−11186.
(48) Kresse, G.; Furthmüller, J. *Comput. Mater. Sci.* **1996**, *6*, 15−50.
(49) Kresse, G.; Hafner, J. *Phys. Rev. B* **1993**, *47*, 558−561.
(50) Payne, M. C.; Makov, G. *Phys. Rev. B* **1995**, *51*, 4014−4022.
(51) Wang, L.; Maxisch, T.; Ceder, G. *Phys. Rev. B* **2006**, *73*, 195107.
(52) Kurth, S.; Perdew, J. P.; Blaha, P. *Int. J. Quantum Chem.* **1999**, *75*, 889.
(53) Hummelshøj, J. S.; Luntz, a C.; Nørskov, J. K. *J. Chem. Phys.* **2013**, *138*, 034703.
(54) Chevrier, V. L.; Ong, S. P.; Armiento, R.; Chan, M. K. Y.; Ceder, G. *Phys. Rev. B* **2010**, *82*, 075122.
(55) Wang, M.; Navrotsky, A. *J. Solid State Chem.* **2005**, *178*, 1230−1240.

DOI: 10.1021/cm503874c
Chem. Mater. 2015, 27, 839−847

(56) *CRC handbook of chemistry and physics*, 93rd ed.; Haynes, W. M., Ed.; CRC Press: Cleveland, OH, 2013.
(57) Colinge, J.-P.; Colinge, C. A. *Physics of semiconductor devices*; Kluwer Academic: Boston, MA, 2002.
(58) Tian, F.; Radin, M. D.; Siegel, D. J. *Chem. Mater.* **2014**, *26*, 2952−2959.
(59) Kang, S.; Mo, Y.; Ong, S. P.; Ceder, G. *Chem. Mater.* **2013**, *25*, 3328−3336.
(60) Radin, M. D.; Rodriguez, J. F.; Siegel, D. J. In *Proceedings of the Battery Congress*; Uddin, M. N., Ed.; Curran Associates, Inc.: Red Hook, NY, 2011.
(61) Lu, Y.-C.; Shao-Horn, Y. *J. Phys. Chem. Lett.* **2013**, *4*, 93−99.
(62) Gallant, B. M.; Kwabi, D. G.; Mitchell, R. R.; Zhou, J.; Thompson, C. V.; Shao-Horn, Y. *Energy Environ. Sci.* **2013**, *6*, 2518.
(63) Khan, A. U.; Mahanti, S. D. *J. Chem. Phys.* **1975**, *63*, 2271.
(64) Zhang, L.; Macdonald, D. D. *Electrochim. Acta* **1998**, *43*, 679−691.
(65) Viswanathan, V.; Thygesen, K. S.; Hummelshøj, J. S.; Nørskov, J. K.; Girishkumar, G.; McCloskey, B. D.; Luntz, A. C. *J. Chem. Phys.* **2011**, *135*, 214704.
(66) Adams, J.; Karulkar, M. *J. Power Sources* **2012**, *199*, 247−255.
(67) Geng, W. T.; He, B. L.; Ohno, T. *J. Phys. Chem. C* **2013**, *117*, 25222−25228.
(68) Felker, F. C.; Kenar, J. A.; Fanta, G. F.; Biswas, A. *Starch* **2013**, *65*, 864−874.
(69) Kosma, V. a.; Beltsios, K. G. *Mater. Sci. Eng., C* **2013**, *33*, 289−297.
(70) Hoang, K.; Johannes, M. D. *J. Power Sources* **2012**, *206*, 274−281.
(71) Meethong, N.; Kao, Y.-H.; Speakman, S. A.; Chiang, Y.-M. *Adv. Funct. Mater.* **2009**, *19*, 1060−1070.
(72) Varley, J. B.; Viswanathan, V.; Nørskov, J. K.; Luntz, A. C. *Energy Environ. Sci.* **2014**, *7*, 720−727.
(73) Zhao, G.; Zhang, L.; Pan, T.; Sun, K. *J. Solid State Electrochem.* **2013**, *17*, 1759−1764.

DOI: 10.1021/cm503874c
Chem. Mater. 2015, 27, 839−847